



Published in final edited form as:

Nat Immunol. 2009 July ; 10(7): 734–743. doi:10.1038/ni.1744.

Macrophage colony stimulating factor induces macrophage proliferation and survival through a pathway involving DAP12 and β -catenin

Karel Otero, Isaiah R Turnbull, Pietro Luigi Poliani*, William Vermi*, Elisa Cerutti, Taiki Aoshi[§], Ilaria Tassi, Toshiyuki Takai[#], Samuel L. Stanley[&], Mark Miller, Andrey S. Shaw, and Marco Colonna

Department of Pathology and Immunology, Washington University School of Medicine, St. Louis, MO 63110, USA

*Department of Pathology, University of Brescia, Spedali Civili, 25123 Brescia, Italy

[#]Department of Experimental Immunology, Japan Science and Technology Agency, Tohoku University, Aoba-ku, Sendai-shi 980-8575, Japan

[&]Division of Infectious Diseases, Department of Medicine, Washington University School of Medicine, St. Louis, MO 63110, USA

Abstract

Macrophage colony stimulating factor (MCSF) influences proliferation and survival of mononuclear phagocytes through the CSF-1 receptor. The DAP12 adaptor protein, which transduces signals emanating from various myeloid receptors, is critical for mononuclear phagocyte function. DAP12-mutant mice and humans show defects in osteoclasts and microglia and exhibit brain and bone abnormalities. Here, we demonstrated that DAP12 deficiency impairs MCSF-induced macrophage proliferation and survival *in vitro*. In addition, DAP12-deficient mice show fewer microglia in defined central nervous system areas, and DAP12-deficient progenitors regenerate myeloid cells inefficiently following BM transplantation. MCSF-CSF1-R signaling induced stabilization and nuclear translocation of β -catenin, which activates cell cycle genes. DAP12 was essential for phosphorylation and nuclear accumulation of β -catenin. These results outline a mechanistic explanation for the multiple defects in DAP12-deficient mononuclear phagocytes.

Introduction

Macrophage colony-stimulating factor (MCSF) (<http://www.signaling-gateway.org/molecule/query?afcsid=A001489>), also known as colony-stimulating factor-1 (CSF-1) (<http://www.signaling-gateway.org/molecule/query?afcsid=A000674>), is the primary regulator of proliferation, survival and differentiation of mononuclear phagocytes, which

Correspondence should be sent to M.C. (mcolonna@pathology.wustl.edu).

[§]Present address: Research Institute for Microbial Diseases, Osaka University. 3-1 Yamada-oka, Suita, Osaka 565-0871, Japan.

The authors declare no conflicting financial interests.

include monocytes, macrophages, bone resorbing osteoclasts and their precursors¹⁻³. MCSF acts through the CSF-1 receptor (CSF-1R), a tyrosine kinase encoded by the *c-fms* proto-oncogene⁴ that is expressed exclusively on mononuclear phagocytes. Binding of MCSF to CSF-1R results in receptor dimerization, autophosphorylation of several tyrosine residues located in the cytoplasmic domain and phosphorylation of many other proteins, including the phosphatase SHP-1, and the kinases Src, PLC- γ , PI3-kinase, AKT and ERK⁵⁻⁸. The MCSF-CSF-1R complex is subsequently internalized and degraded in lysosomes. Signaling through CSF-1R is required for entry of cells into S-phase^{9,10} and for cell survival¹¹. The biological importance of the MCSF-CSF-1R axis is evinced by osteopetrotic (op/op) mice, which lack a functional MCSF gene¹². These mice show osteopetrosis due to impaired osteoclast formation as well as deficits in blood monocytes and tissue macrophages. *In vitro*, MCSF-CSF-1R signaling drives the proliferation and differentiation of precursor cells into macrophages or osteoclasts, and is required for the survival of these cells. However, mononuclear phagocytes are not uniformly dependent on MCSF¹³; whereas some subpopulations continuously require MCSF, others, such as microglia, depend on MCSF only in specific areas of the central nervous system (CNS)¹⁴⁻¹⁶.

DAP12 (<http://www.signaling-gateway.org/molecule/query?afcsid=A000750>) is an adaptor protein associated with several myeloid and lymphocyte receptors; these receptors require DAP12 for cell surface expression and signaling¹⁷. DAP12 consists of a short extracellular and transmembrane region followed by a cytoplasmic domain that contains an immunoreceptor tyrosine-based activation motif (ITAM). Upon engagement of the associated receptor, the DAP12 ITAM is phosphorylated and acts as a docking site for the protein tyrosine kinases Syk and ZAP70, which recruit and activate multiple downstream adaptors and signaling enzymes that induce cell activation. The crucial role of DAP12 and DAP12-associated receptors in the function of mononuclear phagocytes is manifest in a human disease, Nasu-Hakola Disease (NHD), which is caused by a recessive mutation in DAP12 or the associated cell-surface receptor TREM-2^{18,19}. NHD is characterized by brain demyelination and gliosis, which engender presenile dementia, as well as by polycystic osteodysplasia, which causes spontaneous fractures. DAP12 is expressed in microglia and osteoclasts, suggesting that NHD may result from impaired function and/or differentiation of these cells.

Three independent lines of DAP12-deficient mice have been generated, and these mice collectively confirm the function of DAP12 in mononuclear phagocytes. DAP12-deficient mice develop osteopetrosis²⁰⁻²² because DAP12-deficient osteoclast precursors differentiate poorly—primarily due to impaired integrin signaling²³—into osteoclasts^{20-22,24,25}. However, whether microglia is defective in DAP12-deficient mice is unclear. One study of mice expressing an ITAM-less mutant DAP12 reported delayed post-natal differentiation and migration of microglia into the CNS, whereas microglia in adult mice appeared to be normal²². In contrast, a study of DAP12-deficient mice reported no defect of microglia, but abnormal development of oligodendrocytes, hypomyelination and synaptic degeneration²⁰. In addition to osteoclast and microglia defects, DAP12 deficiency also augments cytokine secretion and Erk activation in macrophages in response to microbial stimuli²⁶. However, a

mechanism involving DAP12 that would account for the CNS defect and the skewed macrophage activation has yet to be defined.

Herein, we demonstrated that DAP12-deficient mononuclear phagocytes are less responsive to MCSF *in vitro*; as a result DAP12-deficient phagocytic monocytes show reduced proliferation and survival. *In vivo*, DAP12 deficiency caused a profound reduction in the numbers of microglial cells in certain areas of the CNS of aged mice as well as reduced regeneration of myeloid cells after bone marrow (BM) transplantation. Mechanistically, we demonstrated that CSF1-R signaling involves stabilization, tyrosine phosphorylation and nuclear translocation of β -catenin (<http://www.signaling-gateway.org/molecule/query?afcsid=A000506>), which is essential for subsequent activation of genes that facilitate cell division. Crucially, DAP12 was essential for optimal phosphorylation and nuclear accumulation of β -catenin. Moreover, this process involved the tyrosine kinase Pyk2 (<http://www.signaling-gateway.org/molecule/query?afcsid=A001952>). Skewed MCSF signaling and defective proliferation and survival of DAP12-deficient mononuclear phagocytes may therefore contribute to the pathology observed in NHD patients.

Results

Impaired growth of DAP12-deficient macrophages

During routine culture of wild-type and DAP12-deficient BM cells with MCSF to generate BM-derived macrophages (BMDM), we noted a deficit in the yield of DAP12-deficient compared to wild-type macrophages. To quantify this deficiency, we cultured DAP12-deficient and wild-type BM cells with MCSF for 10 days and counted all viable cells at different time points. In wild-type cultures, the number of BMDM increased until day 7 of culture, and declined at day 10 (Fig. 1a). Since macrophages rapidly degrade MCSF, this decline may reflect consumption of MCSF in the cultures, which results in growth arrest and apoptosis. Importantly, at day 7 and day 10, DAP12-deficient cultures contained significantly fewer cells than wild-type cultures (Fig. 1a).

This reduction could be due to reduced proliferation or increased cell death. To assess the contribution of each of these mechanisms, we collected cells at days 5, 7 and 10 of culture and analyzed cell cycle and cell death by measuring DNA content with propidium iodide (PI). Compared to wild-type BMDM, DAP12-deficient BMDM exhibited significant arrest of cells in G₁ at day 5 and 7 and a small increase in hypodiploid cells that correspond to apoptotic cells (Fig. 1b). These data suggest that DAP12-deficient cells divide less efficiently than wild-type cells in response to MCSF at these time points. In addition, we observed a marked increase in hypodiploid cells in DAP12-deficient but not wild-type cultures at day 10 (Fig. 1b). Thus, DAP12 may be required for both MCSF-dependent macrophage proliferation and survival and its contribution to each process may vary at different culture stages.

DAP12 is needed for MCSF-induced proliferation

To directly measure the impact of DAP12 deficiency on MCSF-induced proliferation, we stimulated wild-type and DAP12-deficient BMDM at day 5 of culture with two different

concentrations of MCSF and analyzed the cell cycle by PI staining. The percentage of DAP12-deficient BMDM in either S or G₂ phase was reduced and the percentage in G₁ phase was increased compared to wild-type BMDM at both MCSF concentrations (Fig. 2a). Retroviral transduction of DAP12 into DAP12-deficient BMDM reconstituted a cell cycle profile similar to that of wild-type cells, directly linking DAP12-deficiency to reduced proliferation (Fig. 2b). We also quantified the proliferation of wild-type and DAP12-deficient BMDM by flow cytometric analysis of 5-bromo-2'-deoxyuridine (BrdU) incorporation. Only 14.6±1.8% of DAP12-deficient cells incorporated BrdU compared to 44.6±2.9% of wild-type cells, further demonstrating a defect in the proliferative response to MCSF in DAP12-deficient cells (Fig. 2c). To confirm the defect in cell cycling, we measured expression of mRNA transcripts encoding cell cycle regulatory proteins in BMDM. Compared to wild-type cells, DAP12-deficient cells expressed less c-Myb mRNA at day 5, and lower amounts of c-Myc, cyclin D1, cyclin D2 mRNA at day 5 and day 7 of culture (Fig. 2d).

To rule out the possibility that DAP12-deficient BMDM proliferate poorly in response to MCSF due to a general defect in macrophage differentiation, we transduced wild-type BMDM with a retrovirus encoding a dominant negative form of DAP12 (DAP12-DN), which lacks a functional ITAM. Expression of DAP12-DN caused a marked cell cycle arrest in G₁ and inhibited BrdU incorporation (Fig. 2e,f). Overall, these data confirm a role for DAP12 in MCSF-driven proliferation.

DAP12 in MCSF-induced macrophage survival

To assess the role of DAP12 in macrophage survival, we deprived BMDM of MCSF for 24 h and measured apoptosis by PI staining. Compared to DAP12-deficient BMDM, wild-type cells were more resistant to apoptosis (Fig. 3a,b). Retroviral transduction of DAP12 into DAP12-deficient BMDM markedly reduced apoptosis, connecting DAP12-deficiency with reduced survival (Fig. 3c).

BMDM cultures contain endogenous MCSF, which is produced by contaminating fibroblast-like stromal cells. Therefore, to precisely quantify the difference in MCSF-induced survival between wild-type and DAP12-deficient BMDM, we generated pure myeloid precursor cultures free of contaminating fibroblast-like stromal cells²⁷. These precursors were seeded in equal numbers in varying amounts of MCSF for 4 days. Pure cultures of wild-type macrophages required exogenous MCSF for survival, and a clear dose-response relationship was observed between the number of cells remaining after 4 days and the dose of MCSF (Fig. 3d). In contrast, DAP12-deficient cultures contained fewer cells than wild-type cultures at all MCSF concentrations.

To confirm that DAP12-deficient macrophages die by apoptosis, BMDM were kept in the presence or absence of MCSF for 16 h, lysed and probed for the presence of active caspase-3 by immunoblotting. We detected no active caspase-3 in lysates of wild-type cells grown with or without MCSF. In contrast, DAP12-deficient cells contained high amounts of active caspase-3 after withdrawal of MCSF (Fig. 3e). Together these experiments demonstrate a quantitative defect in MCSF-induced survival of DAP12-deficient macrophages.

To determine whether wild-type cells produce an extrinsic factor required for survival of BMDM, we assessed survival of wild-type and DAP12-deficient BMDM in co-cultures. BM from DAP12-sufficient transgenic mice expressing GFP was mixed in a 1:1 ratio with BM from wild-type or DAP12-deficient mice, and the cells were co-cultured for 5 days in the presence of MCSF to generate BMDM. Cultures were continued for 2 additional days in the absence of MCSF and, on day 7, the ratio of GFP⁺ to GFP⁻ BMDM was determined. A slight, but reproducible predominance of wild-type (GFP⁻) cells over GFP⁺ cells (58 vs. 42%) was observed in the wild-type:GFP⁺ co-cultures (Fig. 3f), suggesting a slight survival or proliferation advantage of wild-type cells. However, in DAP12-deficient:GFP⁺ BMDM co-cultures, there was a selective loss of almost half of the DAP12-deficient (GFP⁻) cells, such that 71% of the cells remaining in culture were GFP⁺.

We performed similar studies focusing on the related signaling adaptors DAP10 and FcR γ ¹⁷. However, co-culture of BM from DAP10-deficient or FcR γ -deficient mice with GFP⁺ BM suggested that neither DAP10 nor FcR γ influence macrophage proliferation nor survival (Fig. 3f). Taken together, these data indicate that the defect in survival of DAP12-deficient macrophages is specific to DAP12, and, as survival cannot be rescued by a soluble or cell-surface factor present in wild-type cultures, is cell-intrinsic.

Little influence of DAP12 on BMDM differentiation

Since macrophage proliferation and differentiation are coordinately regulated²⁸, we asked whether DAP12-deficiency, while reducing proliferation, accelerates the differentiation of BM cells into mature macrophages *in vitro*. Both DAP12-deficient and wild-type BMDM expressed typical macrophage markers, although DAP12-deficient macrophages expressed lower amounts of CD11b, MHC class II and the scavenger receptors CD36, F4/80 and ApoE, whereas expression of CSF-1R was unchanged (Supplementary Fig. 1, online). Collectively, these observations indicate that lack of DAP12 does not accelerate MCSF-induced differentiation of mature macrophages.

Microglial defects in DAP12-deficient mice

Given the marked defects in DAP12-deficient macrophage proliferation and survival in response to MCSF *in vitro*, we asked whether any abnormality would be manifested *in vivo*. We compared microglia in the brain and the spinal cord of wild-type and DAP12-deficient mice by staining for the microglia marker Iba-1 in young (4 weeks) and aged (10-month-old) mice. We found significantly fewer microglia in the basal ganglia (10.6 ± 3.9 vs. 61.2 ± 8.8 cells / mm²; $P < 0.001$) and the spinal cord (6.2 ± 4.5 vs. 37.3 ± 5.8 cells / mm²; $P < 0.001$) (mean \pm s.d.) of aged DAP12-deficient mice compared to wild-type controls (Fig. 4). Furthermore, at high magnification, we observed extensive cytoplasmic fragmentation (cytorrhesis) and nuclear condensation characteristic of microglial degeneration and apoptotic cell death in the DAP12-deficient animals (Fig. 4). Numbers of microglia were similar in young wild-type and DAP12-deficient mice (data not shown). Additionally, we found no detectable differences between wild-type and DAP12-deficient myelopoiesis, circulating myeloid cells or peripheral macrophages in the spleen and liver (Supplementary Fig. 2 and Supplementary Table 1, online). Based on these observations we conclude that DAP12 is required for long-term preservation of a specific microglia subset.

DAP12 in mononuclear phagocyte repopulation

To compare the generation of DAP12-deficient versus wild-type macrophages *in vivo*, we mixed BM from DAP12-sufficient transgenic mice expressing GFP in a 1:1 ratio with BM from DAP12-deficient (GFP⁻) or wild-type (GFP⁺) mice (Fig. 5a). Mixed BM was then engrafted into lethally irradiated wild-type hosts, resulting in mice in which the GFP⁻ BM was either wild-type (WT:GFP chimeras) or DAP12-deficient (DAP12:GFP chimeras) in origin. These mice were maintained for up to 36 weeks and BM chimerism was evaluated 12, 19 and 36 weeks after engraftment by flow cytometry.

At 12 weeks, the GFP⁺:GFP⁻ ratio of BM in the chimeric mice closely reflected the input ratio (Fig. 5b). At 19 weeks, the proportion of GFP⁺ cells declined (in comparison to input) in the WT:GFP chimeras, suggesting that the wild-type GFP⁻ cells were more robust than the GFP⁺ cells. In contrast, the proportion of GFP⁺ cells remained stable in the DAP12:GFP chimeras, indicating that the DAP12-deficient cells competed less well than wild-type cells *in vivo*, much as they did *in vitro*. At 36 weeks, there was a preponderance of GFP⁻ cells in all chimeras. However, the ratio of GFP⁻ to GFP⁺ cells in the WT:GFP chimeras was significantly greater than that observed in the DAP12:GFP chimeras (Fig. 5b). There was no deficit in the total number of nucleated cells in the BM (WT:GFP and DAP12:GFP chimeras had 2.9 and 2.6×10^7 nucleated cells/femur respectively at 36 weeks, consistent with that found in unmanipulated mice (data not shown)). These findings indicate that changes in the GFP⁺:GFP⁻ cell ratio reflect replacement of GFP⁺ cells by GFP⁻ cells. Cumulatively, these data demonstrate that DAP12-deficient BM cells repopulate the BM of irradiated recipient mice less efficiently than wild-type cells.

We also assessed the peripheral cell populations in the chimeric mice at 36 weeks. We examined blood polymorphonuclear cells (PMN; CD115⁻Gr1^{hi}), blood monocytes (CD115⁺Gr1^{lo-int}), peritoneal B cells (CD19⁺) and peritoneal macrophages (F4/80⁺) (Fig. 5c). The GFP⁻:GFP⁺ ratio of PMN was ~2:1 in the WT:GFP and DAP12:GFP chimeras (Fig. 5d). In contrast, the GFP⁻:GFP⁺ ratio of monocytes in the WT:GFP chimeras was greater than that observed in the DAP12:GFP chimeras (3:1 vs 2:1), similar to that observed in the BM (Fig. 5d). This finding is consistent with defective proliferation and/or survival of DAP12-deficient monocytes and/or macrophages. In the peritoneum, we found no difference in the GFP⁻:GFP⁺ ratio of B cells between WT:GFP and DAP12:GFP chimeras (~2:1) (Fig. 5d). In contrast, there were more peritoneal GFP⁻ macrophages than GFP⁺ macrophages in the WT:GFP chimeras (85% versus 15%) than in DAP12:GFP chimeras (75% versus 25%). Taken together, these results support a role for DAP12 in promoting proliferation and survival of monocytes and/or macrophages *in vivo*.

DAP12-deficiency skews MCSF-induced signaling

The inefficient MCSF-induced proliferation and survival of DAP12-deficient cells implies that DAP12 is involved in MCSF signaling. Previous studies have demonstrated that CSF-1R induces proliferation by activating ERK²⁹. Thus, we asked whether CSF-1R requires DAP12 for activation of ERK and other mitogen-activated protein kinases (MAPK). Wild-type and DAP12-deficient BMDM were stimulated with MCSF for various periods of time and downstream signaling intermediates were studied by immunoblot.

Consistent with prior studies, MCSF induced prompt phosphorylation of ERK, p38 and JNK MAPKs and the downstream target p90rsk in wild-type cells (Fig. 6a and data not shown). DAP12 deficiency did not reduce MAPK activation; in fact we observed a small but reproducible increase of ERK, p38 and p90rsk phosphorylation in DAP12-deficient cells (Fig. 6a), whereas JNK phosphorylation was unchanged (data not shown). Thus, the impaired MCSF-induced proliferation of DAP12-deficient macrophages cannot be accounted for by reduced activation of ERK.

Interestingly, it has been reported that MCSF induces transcriptional activation of the MAPK phosphatase 1 (MKP-1)²⁹, which dephosphorylates ERK and p38³⁰. Since DAP12-deficient macrophages are less responsive to MCSF, we tested whether they express reduced levels of MKP-1 and found that this was indeed the case (Fig. 6a,b). This reduction of MKP-1 expression provides a likely explanation for the paradoxical increase of ERK and p38 phosphorylation observed in DAP12-deficient cells. Although it was previously shown that CSF-1R induces macrophage survival by activating PI-3K-AKT²⁹, we found no difference in MCSF-induced AKT phosphorylation between DAP12-deficient and wild-type cells (Fig. 6a). We conclude that DAP12 controls CSF-1R-induced proliferation and survival through a MAPK-independent pathway.

MCSF, via DAP12, activates β -catenin

Among other pathways known to promote cell growth and inhibit apoptosis, the β -catenin pathway was an attractive candidate because β -catenin, upon nuclear translocation, acts a coactivator of the TCF and LEF transcription factors to induce the transcription of cell cycle genes (e.g. cyclin D1^{31,32} and c-myc³³), which were differentially expressed in wild-type and DAP12-deficient BMDM. Activation of the β -catenin pathway depends on the stabilization of β -catenin and its nuclear translocation³⁴. Stability of β -catenin is negatively regulated by GSK3 β , which phosphorylates Ser and Thr residues of β -catenin and thereby induces its subsequent proteasome-mediated degradation³⁴. Nuclear localization is positively regulated by tyrosine phosphorylation^{35,36}. Immunoblot analysis of lysates of BMDM revealed that MCSF increases β -catenin quantities in wild-type cells, indicating a role for MCSF in regulating β -catenin stability (Fig. 7a). β -catenin expression was also increased in MCSF-stimulated DAP12-deficient cells, although to a lower extent; this finding suggests that DAP12 may influence β -catenin stabilization.

We next asked how MCSF and DAP12 mediate activation of β -catenin. MCSF induced GSK3 β serine 9 (Ser9) phosphorylation in wild-type BMDM (Fig. 7b). Since Ser9 phosphorylation inhibits GSK3 β function, this may explain, at least in part, the MCSF-induced stability of β -catenin. Ser9 GSK3 β phosphorylation was DAP12-independent as it was similar in MCSF-stimulated wild-type and DAP12-deficient BMDM. MCSF also induced Tyr phosphorylation and nuclear translocation of β -catenin in wild-type BMDM (Fig. 7c,d). Notably, MCSF-induced Tyr phosphorylation and nuclear translocation of β -catenin were markedly reduced in DAP12-deficient BMDM (Fig. 7c,d). Upon nuclear translocation, β -catenin activates downstream target genes by interacting with LEF and TCF transcription factors³⁴. To corroborate that MCSF induces nuclear translocation of β -catenin and activation of LEF and TCF, we transduced wild-type and DAP12-deficient BMDM with

a luciferase reporter driven by three LEF/TCF sites. MCSF stimulation activated the reporter in wild-type but not DAP12-deficient cells (Fig. 7e). Additionally, β -catenin nuclear accumulation was greatly reduced in wild-type BMDM transduced with DAP12-DN (Fig. 7f). Collectively, these experiments demonstrate that MCSF activates the β -catenin pathway; and that DAP12 is required for MCSF-induced tyrosine phosphorylation and nuclear translocation of β -catenin.

To validate the role of β -catenin activation in MCSF-induced proliferation of BMDM, we treated wild-type and DAP12-deficient BMDM with the specific GSK β 3 inhibitor SB216763 and measured BMDM proliferation by BrdU incorporation. Inhibition of GSK β 3 promoted MCSF-induced proliferation of BMDM and restored proliferation of DAP12-deficient BMDM to that of wild-type BMDM (Fig. 7g). We conclude that β -catenin activation is crucial for the MCSF-DAP12 pathway that stimulates BMDM proliferation.

Pyk2 links DAP12 to β -catenin Tyr phosphorylation

Next we sought to identify molecular mediator(s) facilitating DAP12-mediated β -catenin Tyr phosphorylation. One plausible candidate is the tyrosine kinase Pyk2 (also called calcium-dependent tyrosine kinase, CADTK). DAP12 activates Pyk2, resulting in enhanced signaling of certain cytokines^{37,38} and Pyk2 mediates β -catenin phosphorylation³⁹. To directly address whether DAP12 induces phosphorylation of β -catenin through Pyk2, we stimulated wild-type and DAP12-deficient BMDM with MCSF and assessed Pyk2 phosphorylation as a measure of activation. MCSF induced Pyk2 phosphorylation much more robustly in wild-type than DAP12-deficient BMDM and this phosphorylation was inhibited in wild-type BMDM expressing DAP12-DN (Fig. 8a,b). Moreover, transduction of wild-type BMDM with DAP12-DN or a dominant negative form of Pyk2, known as CADTK-related non-kinase (CRNK)⁴⁰, prevented Tyr phosphorylation of β -catenin by MCSF (Fig. 8c). Finally, Pyk2 co-precipitated with β -catenin from wild-type but not DAP12-deficient MCSF-stimulated BMDM (Fig. 8d).

To corroborate the role of Pyk2-mediated β -catenin activation in MCSF-DAP12-induced BMDM proliferation, we demonstrated that two pharmacological inhibitors of Pyk2 inhibit MCSF-induced BMDM proliferation and cell cycle progression as assessed by BrdU and PI assays (Fig. 8e). Additionally, transduction of wild-type BMDM with CRNK reduced cell cycle progression and proliferation induced by MCSF (Fig. 8f,g).

MCSF induces activation of the protein tyrosine kinase Syk through DAP12 in osteoclasts⁴¹. Therefore we also evaluated the potential role of Syk in MCSF-induced β -catenin activation. MCSF induced DAP12-dependent tyrosine phosphorylation of Syk in BMDM (Supplementary Fig. 3a, online), but Syk was not present in β -catenin immunoprecipitates (data not shown), suggesting that Syk has no direct role in DAP12-induced β -catenin tyrosine phosphorylation. Since a pharmacological inhibitor of Syk inhibited MCSF-induced BMDM proliferation (Supplementary Fig. 3b, online), it is likely that Syk acts as an upstream activator of the Pyk2- β -catenin pathway.

MCSF activates the DAP12-Pyk2- β -catenin pathway independently of cell attachment

It is well established that stimulation of macrophages with MCSF induces remodeling of the actin cytoskeleton and formation of adhesion structures reflective of integrin activation⁴². Moreover, integrin signaling in macrophages involves DAP12 and Syk⁴³ and mediates a tonic Pyk2 activation that regulates responsiveness to interferon (IFN)- α ³⁷. Thus, MCSF could trigger the DAP12-Pyk2- β -catenin signaling pathway by promoting inside-out integrin activation. To explore this possibility, we first determined whether DAP12-deficient BMDM have adhesion defects. In the absence of MCSF, wild-type and DAP12-deficient BMDM attached equally well to fibronectin under both static and continuous flow conditions (Supplementary Fig. 4, online). However, stimulation of BMDM with MCSF did not further increase adhesion in these assays, probably due to the strong basal ability of BMDM to adhere to fibronectin. Therefore, we investigated MCSF-induced cytoskeleton reorganization and formation of focal complexes in adherent BMDM as an indication of macrophage adhesion and integrin activation. After 12 h of MCSF withdrawal, stimulation of wild-type BMDM with MCSF resulted in marked actin reorganization and cell spreading with the formation of membrane ruffles, lamellipodia and filopodia (Supplementary Fig. 5, online). Virtually identical changes were observed in DAP12-deficient BMDM. Moreover, staining of wild-type and DAP12-deficient BMDM with anti-vinculin revealed similar increases in the number and clustering of focal complexes (Supplementary Fig. 6a, online). MCSF-induced redistribution of the integrin CD11b was also equivalent in wild-type and DAP12-deficient BMDM (Supplementary Fig. 6b, online). Thus, MCSF-induced adhesion and rearrangement of actin cytoskeleton are not noticeably affected by lack of DAP12, at least in BMDM.

If the MCSF-DAP12 pathway to β -catenin activation is independent of integrin signaling, it should occur also when BMDM are in suspension. MCSF stimulation of wild-type and DAP12-deficient BMDM in suspension neither increased their ability to bind a soluble ICAM-1-Fc fusion protein nor enhanced clustering of VLA-4, CD11b or LFA-1 on the cell surface, indicating that MCSF does not activate integrins on BMDM in suspension (data not shown). However, MCSF was equally effective in inducing Pyk2 phosphorylation and increasing β -catenin in wild-type BMDM whether cells were in suspension or attached to plates (Supplementary Fig. 7, online). These results indicate that the MCSF activates the DAP12-Pyk2- β -catenin pathway in a cell attachment-independent fashion.

Discussion

This report demonstrates that DAP12 is essential for CSF-1R signaling, specifically for enhancing proliferation and survival of macrophages in response to MCSF. Mechanistically, DAP12 facilitated Pyk2-mediated Tyr phosphorylation and subsequent nuclear translocation of β -catenin.

DAP12-deficient macrophages proliferated poorly in response to MCSF and did not survive in suboptimal amounts of MCSF *in vitro*. These defects were cell-intrinsic. Importantly, the impaired DAP12-deficient macrophage responses to MCSF *in vitro* had a correlate *in vivo*. Relatively few microglia were present in the basal ganglia and the spinal cord in 10 month-old DAP12-deficient mice, and those remaining had an apoptotic phenotype. In addition,

DAP12-deficient myeloid precursors reconstituted the monocyte and macrophage compartment less effectively than precursors from wild-type mice following BM transplantation.

To date, analysis of DAP12-deficient mouse models has yielded ambiguous results regarding the role of DAP12 in microglia^{20,22}. Our results conclusively demonstrate reduced numbers and diminished survival of microglia in particular areas of 10 month-old DAP12-deficient CNS; these defects may stem from decreased responsiveness to MCSF. Our examination of the basal ganglia and spinal cord in aged mice may have increased the sensitivity of our analysis relative to a previous study of this line of DAP12-deficient mice²⁰.

Interestingly, mononuclear phagocytes do not uniformly rely on MCSF for survival¹³. While osteoclasts and spleen macrophages are entirely MCSF-dependent, microglia require MCSF only in specific areas of the central nervous system (CNS)¹⁴⁻¹⁶. This may explain why DAP12-deficiency exclusively affected microglia in restricted locations within the CNS. Because microglia are critical for local defense and trophism, confined impairment of microglia in a discrete location may predispose the CNS to distinct pathological defects such as those occurring in NHD. It is possible that DAP12 is involved in MCSF-induced proliferation and survival of mononuclear phagocytes other than microglia, but lack of DAP12 may be compensated by continuous supply of MCSF. Future studies will address the contribution DAP12 under conditions in which MCSF is limiting or rapidly consumed.

In addition to reducing proliferation and survival of mononuclear phagocytes, DAP12 deficiency augmented MCSF-induced MAPK activation. Since MCSF induces expression of MKP-1²⁹, impaired responses to MCSF in DAP12-deficient macrophages may result in reduced expression of MKP-1 and consequently increased MAPK phosphorylation. Reduced MKP-1 expression may also explain the increase in ERK activation and cytokine responses to Toll-like receptor agonists previously reported in DAP12-deficient BMDM²⁶.

Notably, we found that CSF-1R activates the β -catenin pathway, which is known to control cell proliferation and survival in other cell types³⁴. Activation of the β -catenin pathway depends on stabilization of β -catenin and its nuclear translocation. We found that MCSF acts on both processes. MCSF induced phosphorylation of Ser9 in GSK3 β , which reduces GSK3 β kinase activity and therefore promotes β -catenin stability. Additionally, MCSF induced Tyr phosphorylation and subsequent nuclear translocation of β -catenin. Although DAP12 had no effect on GSK3 β phosphorylation, it was absolutely required for Tyr phosphorylation and nuclear accumulation of β -catenin. The reduced nuclear translocation of β -catenin in DAP12-deficient BMDM provides a likely explanation for the reduced abundance of cyclin D1 and c-myc mRNA transcripts in these cells compared to wild-type BMDM. Recent studies demonstrate that β -catenin is important for the self-renewal and maintenance of hematopoietic stem cells and myeloid progenitor cell pools⁴⁴. Our results extend these studies, showing that β -catenin is important not only at the stem cell stage, but also at later stages of macrophage population expansion and differentiation, when DAP12 and its associated receptors are expressed. This was particularly evident in the mixed BM

chimera experiments, in which DAP12-deficient BM clearly repopulated irradiated hosts but generated fewer mature monocytes and macrophages than wild-type BM.

Finally, we identify Pyk2 as the tyrosine kinase that links DAP12 to Tyr phosphorylation of β -catenin. Previous studies have described Pyk2 as a downstream signaling intermediate of DAP12^{37,38}, as well as an effector of β -catenin phosphorylation³⁹. Consistent with both observations, we found that MCSF induces Pyk2 activation and association with β -catenin in a DAP12-dependent fashion. The signaling pathway connecting DAP12 and Pyk2 remains to be elucidated. Although MCSF activates cell adhesion and DAP12 is known to be a mediator of integrin signaling⁴³, our data indicate that the MCSF activation of the DAP12-Pyk2- β -catenin pathway is adhesion-independent. Thus, this pathway appears to be distinct from the cell attachment-DAP12-Pyk2 pathway that mediates tonic regulation of IFN- α and interleukin 10 signaling³⁷. A recent study⁴¹ and our own data suggest that MCSF-DAP12 may act through Syk and possibly other kinases that have been implicated in macrophage survival and osteoclast function, such as TEC^{45,46}. In conclusion, our identification of a link between the MCSF, the DAP12 ITAM and β -catenin unveils an unprecedented signaling network regulating proliferation and survival of myeloid cells.

Methods

Mice

All animal studies were approved by the Washington University Animal Studies Committee. B6.129P2-TYROBPtm1Ttk mice (referred to as DAP12-deficient) and B6.129P2-HCSTm1cln (referred to as DAP10-deficient) were previously described^{20,47}. C57BL/6-Tg(UBC-GFP)30Scha/J mice (referred to as GFP⁺) were purchased from Jackson Laboratories. B6.129P2-Fc ϵ r1gtm1Rav mice (referred to as FcR γ -deficient) and wild-type control C57BL/6 mice were purchased from Taconic Laboratories.

DNA constructs

A LEF-luc-pGL3 reporter plasmid was kindly provided by D.M. Ornitz (Department of Developmental Biology, Washington University School of Medicine). A *XhoI-SalI* DNA fragment including 3 LEF sites, the fos promoter and the luciferase gene was subcloned into the *XhoI* site of the retroviral vector pMX⁴⁸ in the 3'-5' orientation with respect to the pMX promoter. A plasmid encoding CRNK, which corresponds to the C-terminal noncatalytic domain of Pyk2, was kindly provided by H.S. Earp III (University of North Carolina Chapel Hill). A DNA fragment encompassing CRNK was subcloned into pMX-ires-GFP⁴⁸. A YFP-tagged DAP12 molecule was constructed and cloned into the pMX retrovirus vector⁴⁹. DAP12-DN was generated from YFP-tagged DAP12 by mutating ITAM tyrosines into phenylalanines as previously described⁵⁰.

Generation and transduction of BMDM

BMDM were differentiated *in vitro* from BM cells cultured in BMDM differentiation media containing 30% L929-cell conditioned media (LCM) as a source of MCSF. At day 5 (or otherwise stated) non-adherent cells were removed and adherent cells used as indicated. For BMDM transduction, retroviral constructs were transiently transfected into Plat-E packaging

cells using FuGENE 6 transfection reagent (Roche). Virus was collected after 2 days and exposed to BMDM at day 3 of culture for 24 h in the presence of 4 µg/ml Polybrene (Sigma). Cells were further cultured in BMDM differentiation media for 1 additional day. At this point, both YFP⁺ (or GFP⁺) and YFP⁻ (or GFP⁻) cells were sorted by FACS, cultured overnight in BMDM differentiation media and then used for experiments. Where indicated, BMDM were derived from a pure population of myeloid precursors, generated as previously described²⁷.

Analysis of cell cycle and apoptosis

Cell cycle and cell death status was determined based on DNA content of cells. Cells were washed with FACS buffer (PBS+2% FCS), fixed with 70% ethanol, and stained with propidium iodide (PI) according to established protocols. Samples were analyzed on a FACStar flow cytometer (BD Biosciences).

Proliferation assay

MCSF-stimulated cells were labeled with 50 µg/ml 5-bromodeoxyuridine (BrdU) for 8 or 20 h, and BrdU incorporation was measured by flow cytometry using a FITC BrdU Flow kit (BD Pharmingen). In some experiments, proliferation and cell cycle analysis were performed in the presence of Pyk2 inhibitors PF431396 (kindly provided by Pfizer) and AG17 (Calbiochem) or the Syk inhibitor (Calbiochem).

RNA isolation and quantitative PCR

Total RNA was extracted from BMDM at different time points during culture using the Trizol reagent (Invitrogen) according to manufacturer's instructions. After first-strand cDNA synthesis using a SuperScript first-strand synthesis system for RTPCR (Invitrogen), real-time quantitative PCR reactions were performed on a Biorad I-Cycler. Reactions were set up using an iQTM SYBR Green supermix (Biorad) and specific primers (Supplementary Table 2, online). Relative quantification of target mRNA expression was calculated and normalized to the expression of *Hprt1* and expressed as (mRNA of the target gene / *Hprt1* mRNA) × 10⁶.

CNS histology

Four animals per group (wild-type and DAP12-deficient) were sacrificed at 10 months after birth. Brains and spinal cords were removed and fixed overnight in 4% paraformaldehyde. Tissue samples were embedded in paraffin and 4µm sections were cut and stained for histological examination. Routine haematoxylin and eosin staining were used to study basic histopathological changes. Immunohistochemistry was used to investigate the microglia morphology and distribution. Briefly, sections were de-waxed, re-hydrated and endogenous peroxidase activity was blocked with 0.3% H₂O₂ in methanol for 15 min. Microwave treatment in 1.0 mM EDTA buffer pH 8.0 was used for epitope retrieval. The sections were then washed, pre-incubated in blocking buffer containing 5% normal goat serum in Tris-HCl for 5 min and incubated for 2 h with polyclonal rabbit anti-Iba-1 primary antibody (1:500, Wako-Chem) in Tris-1% BSA. Sections were then washed in Tris-HCl buffer prior to incubation for 30 min with the secondary antibody (ChemMATE Envision

Rabbit/Mouse, DAKO Cytomation). Signal was revealed with diaminobenzidine (DAB) and slides counterstained with hematoxylin. Images were taken with Olympus DP70 camera mounted on Olympus Bx60 microscope using Cell-F imaging software (Soft Imaging System GmbH). Quantification was performed on five different representative spinal cord and brain sections for each animal counting the number of Iba-1 positive cells present in each area. Results were expressed as mean \pm s.d. of positive cells/mm².

Immunoprecipitation and immunoblotting

BMDM were cultured in medium without LCM for 4 h and then collected and replated onto non-tissue culture plates. Cells were stimulated with mouse MCSF (R&D Systems) for the appropriate times and lysed in a buffer containing 1% NP-40 and inhibitors as described previously⁴⁹. For immunoprecipitation of β -catenin, 200 μ g of cell lysates were immunoprecipitated with anti- β -catenin (9562, Cell Signaling Technology) and protein A Sepharose (GE Healthcare). Cell lysates were separated by standard SDS-PAGE and analyzed by immunoblotting. Antibodies directed to the following molecules were used: active caspase 3 (9661), phospho-ERK (9101), phospho-p90RSK (9344), p38 (9212), phospho38 (9211), Akt (9272), phospho-Akt (9271), phospho-GSK-3 β -Ser9 (9336), JNK (9252), phospho-JNK (9251), Syk (2712), β -catenin (9562) and GAPDH (14C10) (all from Cell Signaling Technology); phospho-tyrosine (4G10, Upstate); ERK-2 (C-14), β -actin (C-11), Syk (N-19), MKP-1 (V-15) and Lamin B (C-20) (all from Santa Cruz Biotechnology); phospho-Pyk2 (44-632, BioSource) and Pyk2 (610548, BD Transduction labs).

BM chimeras

Recipient mice were irradiated with 950 rads of γ -irradiation to ablate endogenous BM. Donor BM was isolated from the femurs and tibia of mice and the red blood cells lysed with RBC lysis buffer (Sigma). CD4⁺ and CD8⁺ T cells were eliminated by incubation with anti-CD4 IgM (RL172) and anti-CD8 IgM (31M) in PBS + 5% BSA for 20 min at 37°C, followed by addition of 1 mL of rabbit complement (Cedar Lane) and incubation for an additional 45 min at 37°C. Cells were washed twice with PBS + 5% BSA, resuspended in DMEM and 10⁷ cells were transferred to each host mouse intravenously.

Supplementary Material

Refer to Web version on PubMed Central for supplementary material.

Acknowledgments

This work was supported by grants R01 GM077279 (M.C.), U54 AI1057160 (S.L.S.), Nobel Project Fondazione Cariplo (W.V.) and Fondazione Nocivelli (P.L.P.). We thank S. Gilfillan for critically reading the manuscript, C. Laudanna and B. Rossi for advise on cell adhesion experiments and Pfizer for the Pyk2 inhibitor.

References

1. Stanley ER, et al. Biology and action of colony-stimulating factor-1. *Mol Reprod Dev.* 1997; 46:4–10. [PubMed: 8981357]

2. Chitu V, Stanley ER. Colony-stimulating factor-1 in immunity and inflammation. *Curr Opin Immunol.* 2006; 18:39–48. [PubMed: 16337366]
3. Hamilton JA. Colony-stimulating factors in inflammation and autoimmunity. *Nat Rev Immunol.* 2008; 8:533–44. [PubMed: 18551128]
4. Sherr CJ, et al. The c-fms proto-oncogene product is related to the receptor for the mononuclear phagocyte growth factor, CSF-1. *Cell.* 1985; 41:665–76. [PubMed: 2408759]
5. Downing JR, Rettenmier CW, Sherr CJ. Ligand-induced tyrosine kinase activity of the colony-stimulating factor 1 receptor in a murine macrophage cell line. *Mol Cell Biol.* 1988; 8:1795–9. [PubMed: 2837654]
6. Sengupta A, et al. Identification and subcellular localization of proteins that are rapidly phosphorylated in tyrosine in response to colony-stimulating factor 1. *Proc Natl Acad Sci U S A.* 1988; 85:8062–6. [PubMed: 2460861]
7. Hamilton JA. CSF-1 signal transduction. *J Leukoc Biol.* 1997; 62:145–55. [PubMed: 9261328]
8. Yeung YG, Stanley ER. Proteomic approaches to the analysis of early events in colony-stimulating factor-1 signal transduction. *Mol Cell Proteomics.* 2003; 2:1143–55. [PubMed: 12966146]
9. Tushinski RJ, Stanley ER. The regulation of mononuclear phagocyte entry into S phase by the colony stimulating factor CSF-1. *J Cell Physiol.* 1985; 122:221–8. [PubMed: 3871440]
10. Roussel MF. Regulation of cell cycle entry and G1 progression by CSF-1. *Mol Reprod Dev.* 1997; 46:11–8. [PubMed: 8981358]
11. Tushinski RJ, et al. Survival of mononuclear phagocytes depends on a lineage-specific growth factor that the differentiated cells selectively destroy. *Cell.* 1982; 28:71–81. [PubMed: 6978185]
12. Wiktor-Jedrzejczak W, et al. Total absence of colony-stimulating factor 1 in the macrophage-deficient osteopetrotic (op/op) mouse. *Proc Natl Acad Sci U S A.* 1990; 87:4828–32. [PubMed: 2191302]
13. Cecchini MG, et al. Role of colony stimulating factor-1 in the establishment and regulation of tissue macrophages during postnatal development of the mouse. *Development.* 1994; 120:1357–72. [PubMed: 8050349]
14. Kondo Y, Lemere CA, Seabrook TJ. Osteopetrotic (op/op) mice have reduced microglia, no Abeta deposition, and no changes in dopaminergic neurons. *J Neuroinflammation.* 2007; 4:31. [PubMed: 18093340]
15. Wegiel J, et al. Reduced number and altered morphology of microglial cells in colony stimulating factor-1-deficient osteopetrotic op/op mice. *Brain Res.* 1998; 804:135–9. [PubMed: 9729335]
16. Witmer-Pack MD, et al. Identification of macrophages and dendritic cells in the osteopetrotic (op/op) mouse. *J Cell Sci.* 1993; 104(Pt 4):1021–9. [PubMed: 8314887]
17. Lanier LL. DAP10- and DAP12-associated receptors in innate immunity. *Immunol Rev.* 2009; 227:150–60. [PubMed: 19120482]
18. Paloneva J, et al. Loss-of-function mutations in TYROBP (DAP12) result in a presenile dementia with bone cysts. *Nat Genet.* 2000; 25:357–61. [PubMed: 10888890]
19. Paloneva J, et al. Mutations in two genes encoding different subunits of a receptor signaling complex result in an identical disease phenotype. *Am J Hum Genet.* 2002; 71:656–62. [PubMed: 12080485]
20. Kaifu T, et al. Osteopetrosis and thalamic hypomyelinoses with synaptic degeneration in DAP12-deficient mice. *J Clin Invest.* 2003; 111:323–32. [PubMed: 12569157]
21. Humphrey MB, et al. The signaling adapter protein DAP12 regulates multinucleation during osteoclast development. *J Bone Miner Res.* 2004; 19:224–34. [PubMed: 14969392]
22. Nataf S, et al. Brain and bone damage in KARAP/DAP12 loss-of-function mice correlate with alterations in microglia and osteoclast lineages. *Am J Pathol.* 2005; 166:275–86. [PubMed: 15632019]
23. Zou W, et al. Syk, c-Src, the alphavbeta3 integrin, and ITAM immunoreceptors, in concert, regulate osteoclastic bone resorption. *J Cell Biol.* 2007; 176:877–88. [PubMed: 17353363]
24. Paloneva J, et al. DAP12/TREM2 deficiency results in impaired osteoclast differentiation and osteoporotic features. *J Exp Med.* 2003; 198:669–75. [PubMed: 12925681]

25. Faccio R, Zou W, Colaianni G, Teitelbaum SL, Ross FP. High dose M-CSF partially rescues the Dap12^{-/-} osteoclast phenotype. *J Cell Biochem.* 2003; 90:871–83. [PubMed: 14624447]
26. Hamerman JA, Tchao NK, Lowell CA, Lanier LL. Enhanced Toll-like receptor responses in the absence of signaling adaptor DAP12. *Nat Immunol.* 2005; 6:579–86. [PubMed: 15895090]
27. Stanley ER. Murine bone marrow-derived macrophages. *Methods Mol Biol.* 1997; 75:301–4. [PubMed: 9276279]
28. Klappacher GW, et al. An induced Ets repressor complex regulates growth arrest during terminal macrophage differentiation. *Cell.* 2002; 109:169–80. [PubMed: 12007404]
29. Xaus J, et al. Molecular mechanisms involved in macrophage survival, proliferation, activation or apoptosis. *Immunobiology.* 2001; 204:543–50. [PubMed: 11846217]
30. Owens DM, Keyse SM. Differential regulation of MAP kinase signalling by dual-specificity protein phosphatases. *Oncogene.* 2007; 26:3203–13. [PubMed: 17496916]
31. Tetsu O, McCormick F. Beta-catenin regulates expression of cyclin D1 in colon carcinoma cells. *Nature.* 1999; 398:422–6. [PubMed: 10201372]
32. Shtutman M, et al. The cyclin D1 gene is a target of the beta-catenin/LEF-1 pathway. *Proc Natl Acad Sci U S A.* 1999; 96:5522–7. [PubMed: 10318916]
33. He TC, et al. Identification of c-MYC as a target of the APC pathway. *Science.* 1998; 281:1509–12. [PubMed: 9727977]
34. Clevers H. Wnt/beta-catenin signaling in development and disease. *Cell.* 2006; 127:469–80. [PubMed: 17081971]
35. Lilien J, Balsamo J. The regulation of cadherin-mediated adhesion by tyrosine phosphorylation/dephosphorylation of beta-catenin. *Curr Opin Cell Biol.* 2005; 17:459–65. [PubMed: 16099633]
36. Piedra J, et al. Regulation of beta-catenin structure and activity by tyrosine phosphorylation. *J Biol Chem.* 2001; 276:20436–43. [PubMed: 11279024]
37. Wang L, et al. ‘Tuning’ of type I interferon-induced Jak-STAT1 signaling by calcium-dependent kinases in macrophages. *Nat Immunol.* 2008; 9:186–93. [PubMed: 18084294]
38. Hu X, Chen J, Wang L, Ivashkiv LB. Crosstalk among Jak-STAT, Toll-like receptor, and ITAM-dependent pathways in macrophage activation. *J Leukoc Biol.* 2007; 82:237–43. [PubMed: 17502339]
39. van Buul JD, Anthony EC, Fernandez-Borja M, Burrige K, Hordijk PL. Proline-rich tyrosine kinase 2 (Pyk2) mediates vascular endothelial-cadherin-based cell-cell adhesion by regulating beta-catenin tyrosine phosphorylation. *J Biol Chem.* 2005; 280:21129–36. [PubMed: 15778498]
40. Li X, Dy RC, Cance WG, Graves LM, Earp HS. Interactions between two cytoskeleton-associated tyrosine kinases: calcium-dependent tyrosine kinase and focal adhesion tyrosine kinase. *J Biol Chem.* 1999; 274:8917–24. [PubMed: 10085136]
41. Zou W, Reeve JL, Liu Y, Teitelbaum SL, Ross FP. DAP12 couples c-Fms activation to the osteoclast cytoskeleton by recruitment of Syk. *Mol Cell.* 2008; 31:422–31. [PubMed: 18691974]
42. Pixley FJ, Stanley ER. CSF-1 regulation of the wandering macrophage: complexity in action. *Trends Cell Biol.* 2004; 14:628–38. [PubMed: 15519852]
43. Mocsai A, et al. Integrin signaling in neutrophils and macrophages uses adaptors containing immunoreceptor tyrosine-based activation motifs. *Nat Immunol.* 2006; 7:1326–33. [PubMed: 17086186]
44. Scheller M, et al. Hematopoietic stem cell and multilineage defects generated by constitutive beta-catenin activation. *Nat Immunol.* 2006; 7:1037–47. [PubMed: 16951686]
45. Melcher M, et al. Essential roles for the Tec family kinases Tec and Btk in M-CSF receptor signaling pathways that regulate macrophage survival. *J Immunol.* 2008; 180:8048–56. [PubMed: 18523268]
46. Shinohara M, et al. Tyrosine kinases Btk and Tec regulate osteoclast differentiation by linking RANK and ITAM signals. *Cell.* 2008; 132:794–806. [PubMed: 18329366]
47. Gilfillan S, Ho EL, Cella M, Yokoyama WM, Colonna M. NKG2D recruits two distinct adapters to trigger NK cell activation and costimulation. *Nat Immunol.* 2002; 3:1150–5. [PubMed: 12426564]
48. Kitamura T, et al. Retrovirus-mediated gene transfer and expression cloning: powerful tools in functional genomics. *Exp Hematol.* 2003; 31:1007–14. [PubMed: 14585362]

49. Giurisato E, et al. Phosphatidylinositol 3-kinase activation is required to form the NKG2D immunological synapse. *Mol Cell Biol.* 2007; 27:8583–99. [PubMed: 17923698]
50. Chen X, et al. A critical role for DAP10 and DAP12 in CD8+ T cell-mediated tissue damage in large granular lymphocyte leukemia. *Blood.* 2008

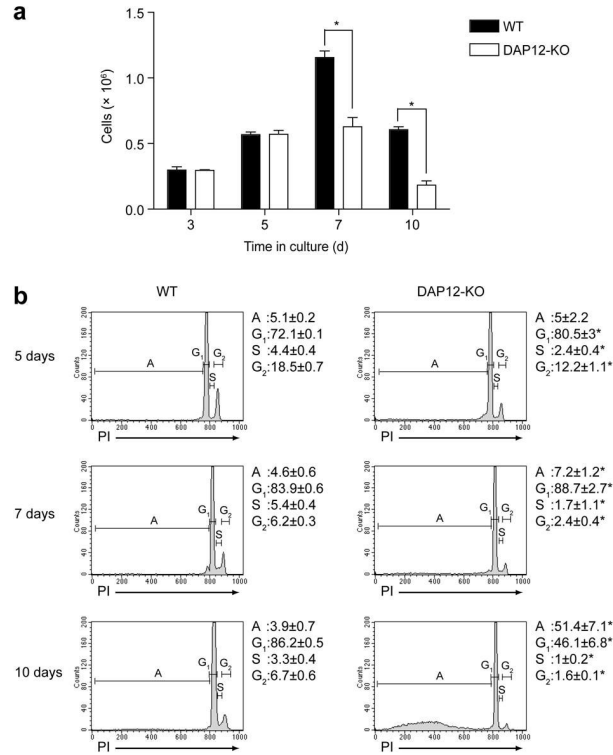


Figure 1. Reduced yield of DAP12-deficient BMDM cultures

(a) BMDM numbers were measured at indicated time points of culture of wild-type and DAP12-deficient BM cells with MCSF (mean and s.d.). *, $P < 0.01$ (Student's t-test). (b) Propidium iodide (PI) analysis of the cell cycle and apoptosis of BMDM cultures at day 5, 7 and 10. Apoptotic cells (A, defined by cells with $<2N$ DNA) and cells in the G₁, S and G₂ phases of the cell cycle were gated, and the percentage of total cells \pm s.d. in each gate is indicated. *, $P < 0.05$ compared to wild-type at the same day of culture (Student's t-test). Data are representative of three separate experiments each including two wild-type and two DAP12-deficient cultures.

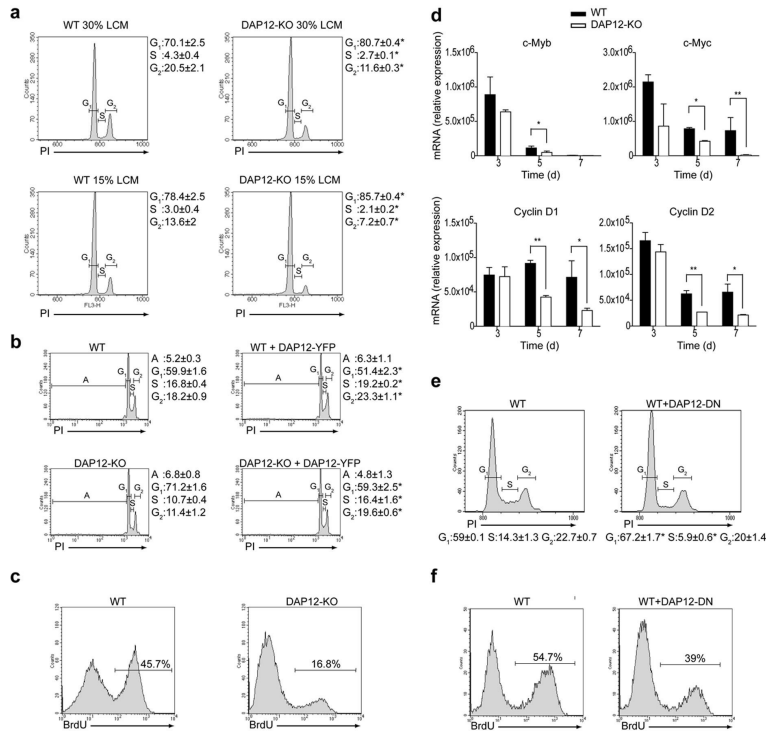


Figure 2. Impaired proliferation of DAP12-deficient BMDM at day 5 of culture

(a) Cell cycle status of wild-type and DAP12-deficient BMDM was measured by PI analysis 24 h after stimulation with 30% or 15% of L929-cell conditioned media (LCM) as a source of MCSF. The percentage of total cells ± s.d. in each gate is marked besides each histogram. *, $P < 0.05$ (Student's t-test) **(b)** BMDM were transduced with retrovirus encoding DAP12-YFP at day 3 of culture. YFP⁺ and YFP⁻ cells were sorted 2 days later, re-plated and cultured for 24 h in medium containing 30% LCM. Cell cycle status was analyzed by PI staining as in **a**. **(c)** Proliferation of wild-type and DAP12-deficient BMDM was measured 24 h after incubation with BrdU in the presence of 30% LCM. **(d)** Expression of indicated mRNA transcripts in wild-type and DAP12-deficient BMDM were measured by real-time PCR at the indicated time of culture (mean and s.d.). *, $P < 0.05$, **, $P < 0.01$. (Student's t-test) **(e,f)** wild-type BMDM were transduced with retrovirus encoding dominant negative DAP12-YFP (DAP12-DN) for 24 h. YFP⁺ and YFP⁻ cells were sorted, re-plated and cultured in medium containing 30% LCM. PI analysis of the cell cycle **(e)** and proliferation by BrdU incorporation **(f)** were assessed after 24 h. Data is representative of three **(a,c,d)** or two **(b,e,f)** experiments.

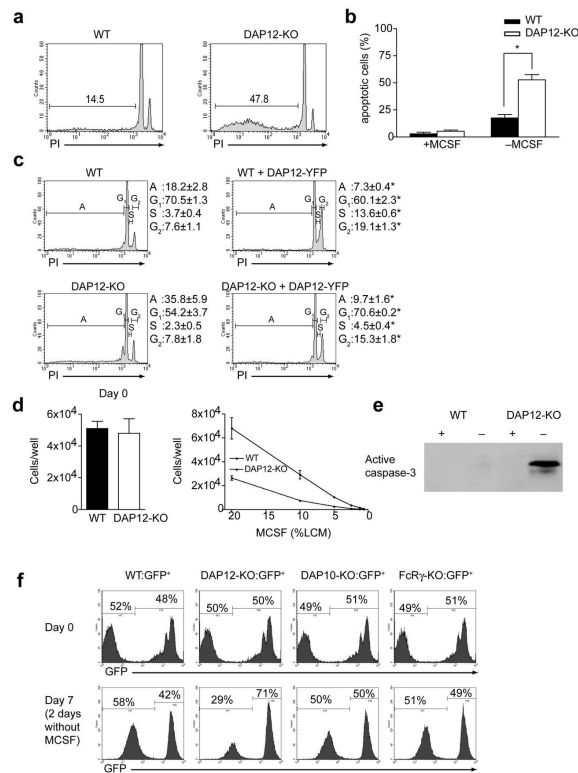


Figure 3. Impaired survival of DAP12-deficient BMDM

(a) Representative histograms showing the percentage of apoptotic wild-type and DAP12-deficient BMDM after 24 h of MCSF deprivation. Numbers in histograms indicate percentage of hypodiploid (<2N DNA) cells, as measured by PI assay. (b) Cumulative percentages of apoptotic BMDM before and after MCSF deprivation (mean and s.d.). *, $P < 0.01$ (Student's t-test) (c) BMDM were transduced with retrovirus encoding DAP12-YFP at day 3 of culture as described in Fig. 2. YFP⁺ and YFP⁻ cells were cultured for additional 24 h without MCSF. The percentage of total cells \pm s.d. in each gate is marked below each histogram. *, $P < 0.05$ (Student's t-test). (d) Pure cultures of myeloid precursors were generated as described in ref 27, then seeded at 10^5 cells/ml into 24 well plates, and cultured with MCSF for 48 h. Nonadherent cells were removed and the number of adherent macrophages enumerated (bar graph, day 0). Macrophages were cultured for 4 additional days in the indicated amount of LCM as a source of MCSF and the number of cells remaining was enumerated (mean and s.d.). (e) BMDM were cultured in the presence or absence of MCSF for 16 h; cell lysates were analyzed for the presence of cleaved (active) caspase-3 by immunoblotting. (f) GFP⁺ (wild-type) and GFP⁻ wild-type (WT), DAP12-KO, DAP10-KO or FcR γ -KO BM cells were mixed in a 1:1 ratio and co-cultured for 5 days in the presence of MCSF, followed by 2 days without MCSF. On day 7 the GFP⁺:GFP⁻ ratio was determined. Data are representative of five (a,b), two (c) or three (d-f) independent experiments.

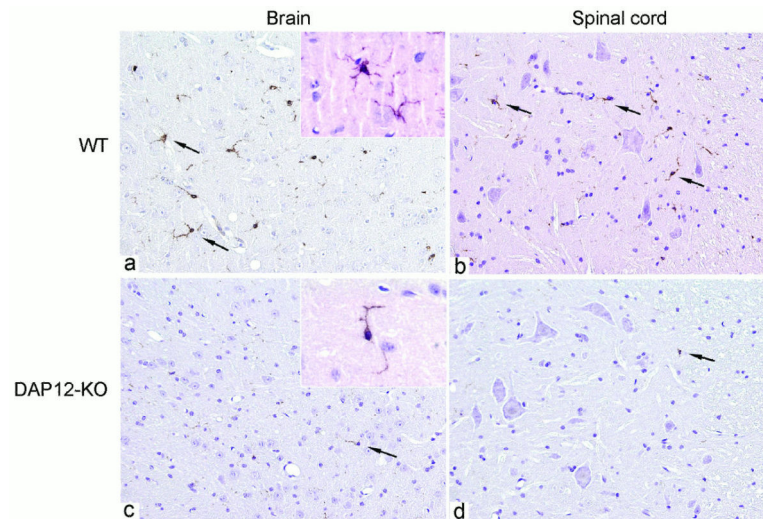


Figure 4. Loss of microglia in CNS of DAP12-deficient mice

Immunohistochemical staining with the Iba-1 microglial marker in representative sections from the basal ganglia brain region (**a,c**) and spinal cord (**b,d**) of 10-month-old wild-type (**a,b**) and DAP12-deficient (**c,d**) mice. Arrows indicate some representative microglial cells. All panels are original 20× magnification and insets are original 60× magnification.

Representative sections from one experiment with four mice per group are shown.

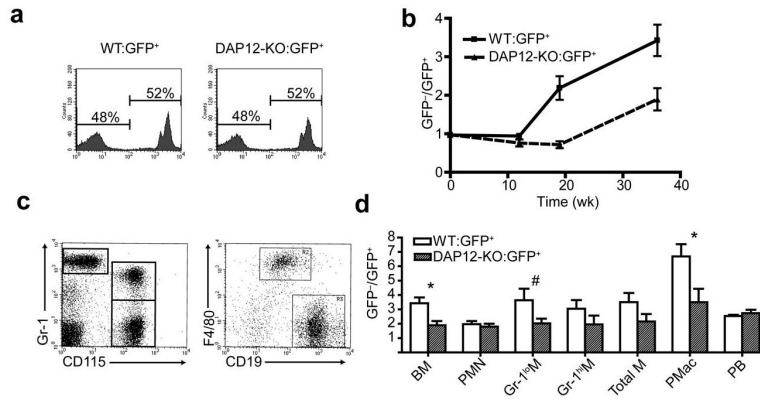


Figure 5. Defect in BM repopulation by DAP12-deficient cells

(a) BM from wild-type or DAP12-deficient mice was mixed 1:1 with BM from DAP12-sufficient GFP⁺ mice as shown in the histograms and adoptively transferred into irradiated wild-type hosts. (b) The GFP⁻:GFP⁺ ratio in the BM of chimeras was determined after 12, 19 or 36 weeks of chimerism (mean and s.d.; $n = 2-3$ for 12 and 19 weeks, $n = 6-7$ for 36 weeks). (c) Identification of peripheral cell populations in mixed BM chimeras. Circulating PMN and monocytes (M) were identified by CD115⁻Gr1^{hi} and CD115⁺Gr1⁺ surface phenotypes, respectively. Peritoneal B cells (PB) were identified by CD19⁺ cells and peritoneal macrophages (PMac) by F4/80⁺ phenotypes. (d) GFP⁻:GFP⁺ ratio in leukocyte populations from WT:GFP and DAP12-KO:GFP chimeras after 36 weeks of chimerism. Data are mean and s.d. of 4-7 individual mice; *, $P < 0.05$; #, $P = 0.06$ (Student's t-test).

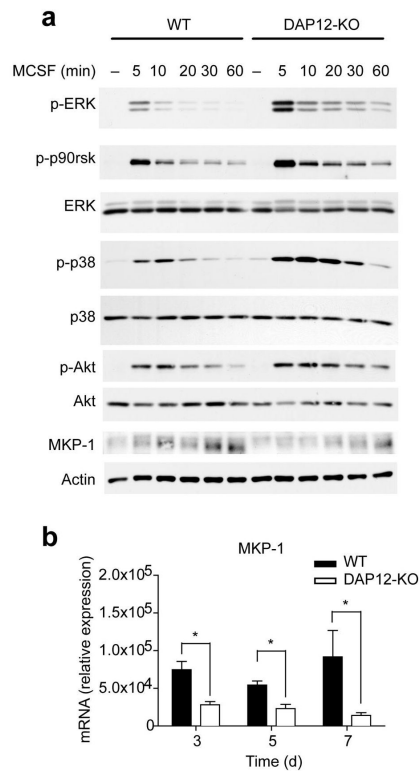


Figure 6. DAP12-deficiency augments MCSF-induced MAPK activation

(a) BMDM were starved of MCSF for 4 h and then restimulated with MCSF (50 ng/ml). After the indicated times total cell lysates were prepared and subjected to immunoblot analysis using antibodies to the indicated phosphorylated proteins. To normalize the data the membranes were stripped and reprobed for the corresponding total proteins or actin. (b) BMDM were cultured in MCSF. At indicated times, cells were lysed and MKP-1 mRNA transcripts were measured by real-time PCR (mean and s.d.). *, $P < 0.01$ (Student's t-test). Data are representative of three to five experiments.

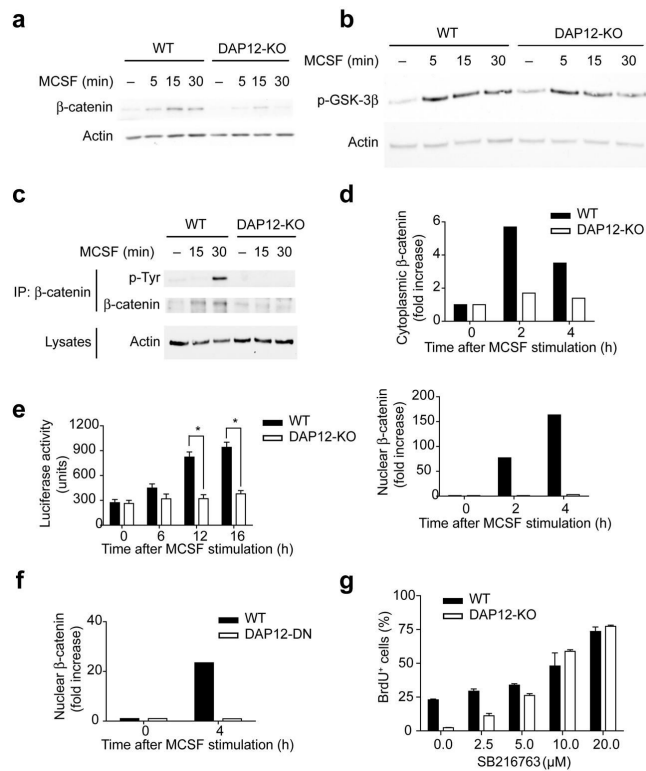


Figure 7. MCSF activates the β -catenin signaling pathway in a DAP12-dependent manner

(a) BMDM were stimulated with MCSF (50 ng/ml) for the indicated times and total cell lysates were analyzed by immunoblotting with anti- β -catenin and anti-actin. (b) Cell lysates were obtained as described in a and analyzed by immunoblotting with anti-phospho-GSK-3 β Ser9 and anti-actin. (c) BMDM were treated with MCSF and cell lysates were subjected to immunoprecipitation (IP) with β -catenin-specific antibodies, followed by immunoblotting with antibodies to phosphotyrosine and β -catenin. Total cell lysates prior to IP were immunoblotted with anti-actin to control for protein amounts. (d) Cells were treated with MCSF and at indicated time points were lysed and divided into nuclear and cytoplasmic fractions. Graphs show densitometric analysis of β -catenin signals corrected for the quantities of housekeeping proteins (GAPDH for cytoplasmic fractions, lamin-B for nuclear fractions). (e) Cells were transduced with a retrovirus encoding a LEF/TCF-luciferase reporter and were stimulated with MCSF for the indicated time periods. (f) wild-type BMDM were transduced with retrovirus encoding dominant negative DAP12-YFP (DAP12-DN) and were stimulated with MCSF for the indicated time points. β -catenin nuclear accumulation was measured as in d. (g) BMDM were cultured in medium containing LCM 30% and BrdU in the presence of varying concentrations of the specific GSK-3 β inhibitor SB216763 for 8 h, and the percentage of BrdU⁺ cells was assessed by FACS (mean and s.d.). *, $P < 0.05$ (Student's t-test). Results are representative of three (a-c) or two (d-g) experiments.

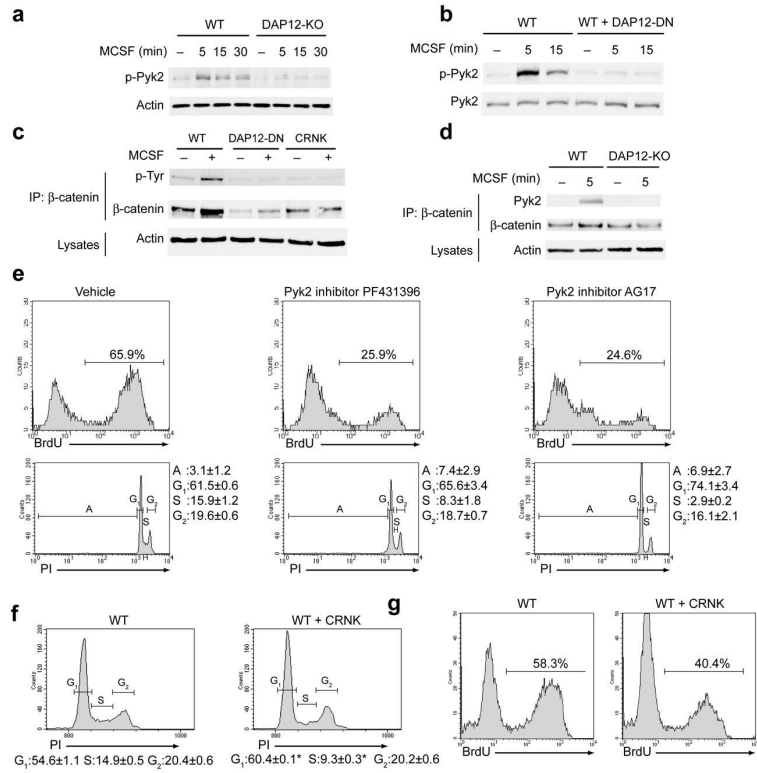


Figure 8. DAP12-mediated tyrosine phosphorylation of β-catenin involves Pyk2

(a,b) wild-type and DAP12-deficient BMDM or wild-type BMDM transduced with retrovirus encoding dominant negative DAP12 (DAP12-DN) were stimulated with MCSF (50 ng/ml). After the indicated times total cell lysates were subjected to immunoblotting analysis using antibodies to phosphorylated Pyk2. To normalize the data the membranes were reprobed for actin or total Pyk2. (c) wild-type BMDM were transduced with retroviruses encoding DAP12-DN or dominant negative Pyk2 (CRNK). Transduced cells were treated or not with MCSF 50 ng/ml for 5 min, total cell lysates were IP with antibodies to β-catenin and immunoblotted with antibodies to phosphotyrosine and β-catenin. Total cell lysates prior to IP were immunoblotted with anti-actin to control for protein amounts. (d) BMDM were stimulated with MCSF as in panel a. After 5 min, whole cell lysates were prepared and IP with anti-β-catenin, followed by immunoblotting analysis with Pyk2 or β-catenin-specific antibodies. Total cell lysates prior to IP were immunoblotted with anti-actin to control for protein amounts. (e) wild-type BMDM were cultured for 8 h in medium containing MCSF (LCM 15%) in the presence or not of the Pyk2 inhibitors PF431396 or AG17 (both at 5 μM). At the end of the incubation, BrdU incorporation (top) or cell cycle analysis (PI; bottom) was assessed. (f,g) Wild-type BMDM transduced with retrovirus encoding CRNK were cultured in medium containing MCSF for 24 h. PI analysis of the cell cycle (f) and BrdU incorporation (g) were assessed after 24 h. Data in e,f are mean ± s.d., *, *P* < 0.05 (Student's t-test). Data are representative of three (a) or two (b-g) experiments.